Research paper

Digoxin net secretory transport in bronchial epithelial cell layers is not exclusively mediated by P-glycoprotein/MDR1 ☆

Victoria Hutter [a,1], David Y.S. Chau [b], Constanze Hilgendorf [c], Alan Brown [d], Anne Cooper [e], Vanessa Zann [e], David I. Pritchard [d], Cynthia Bosquillon [a,*]

[a] Division of Drug Delivery and Tissue Engineering, School of Pharmacy, University of Nottingham, UK
[b] Allergy Research Group, School of Molecular Medical Sciences, University of Nottingham, UK
[c] AstraZeneca R&D, Mölndal, Sweden
[d] Immune Modulation Group, Division of Molecular and Cellular Science, School of Pharmacy, University of Nottingham, UK
[e] AstraZeneca R&D Charnwood, Loughborough, UK

ARTICLE INFO

ABSTRACT

The impact of P-glycoprotein (MDR1, ABCB1) on drug disposition in the lungs as well as its presence and activity in in vitro respiratory drug absorption models remain controversial to date. Hence, we characterised MDR1 expression and the bidirectional transport of the common MDR1 probe ^{3}H-digoxin in air–liquid interfaced (ALI) layers of normal human bronchial epithelial (NHBE) cells and of the Calu-3 bronchial epithelial cell line at different passage numbers. Madin–Darby Canine Kidney (MDCKII) cells transfected with the human MDR1 were used as positive controls. ^{3}H-digoxin efflux ratio (ER) was low and highly variable in NHBE layers. In contrast, ER = 11.4 or 3.0 were measured in Calu-3 layers at a low or high passage number, respectively. These were, however, in contradiction with increased MDR1 protein levels observed upon passaging. Furthermore, ATP depletion and the two MDR1 inhibitory antibodies MRK16 and UIC2 had no or only a marginal impact on ^{3}H-digoxin net secretory transport in the cell line. Our data do not support an exclusive role of MDR1 in ^{3}H-digoxin apparent efflux in ALI Calu-3 layers and suggest the participation of an ATP-independent carrier. Identification of this transporter might provide a better understanding of drug distribution in the lungs.

© 2013 The Authors. Published by Elsevier B.V. All rights reserved.

1. Introduction

Compared to the gastro-intestinal tract, kidney, liver or brain, the expression and functionality of drug transporters remain poorly characterised in the lung, which renders pulmonary drug absorption data challenging to interpret [1,2]. Since the epithelium is the major permeability barrier in the lung, in vitro respiratory epithelial cell culture models have been employed to enhance understanding of the role of active transport mechanisms in the disposition of inhaled drugs [1,3]. In absence of a convenient and truly representative model of the alveolar epithelium, bronchial systems have been favoured [3,4]. Among these, the human bronchial cell line Calu-3 and normal human bronchial epithelial

(NHBE) cells are gaining in popularity due to their capacity to develop polarised cell layers morphologically similar to the native epithelium and suitability for permeability measurements when cultured at an air–liquid interface (ALI) [4–6]. However, although the presence of active drug transport mechanisms has been confirmed in Calu-3 and NHBE layers [1,6–9], an overview of the range of transporters being expressed and functional in these models is still lacking.

P-glycoprotein/multidrug resistance protein 1 (P-gp/MDR1) is a member of the ATP-binding cassette (ABC) efflux transporter family and plays a major role in drug–drug interactions [10], limitation of oral drug absorption and poor drug penetration in the central nervous system [11]. As it has been reported several drugs administered by the pulmonary route might be MDR1 substrates [1], targeting the transporter present in the epithelium has been envisaged as a strategy to increase the residence time of inhaled drugs in the lung tissue. Consequently, MDR1 is by far the most extensively studied drug transporter in the lung [1]. Although weakly expressed in the lung as compared to other major organs [12], the presence of the MDR1 protein has been demonstrated in the bronchial epithelium [1]. However, its actual impact on the pulmonary absorption of established substrates is a matter of

* Corresponding author. Centre for Biomolecular Sciences, University Park, University of Nottingham, Nottingham NG7 2RD, UK. Tel.: +44 115 84 66078; fax: +44 115 95 15122.
E-mail address: cynthia.bosquillon@nottingham.ac.uk (C. Bosquillon).
[1] Present address: Department of Pharmacy, University of Hertfordshire, UK.

debate [1]. Similarly, reports on the expression, localisation and functionality of MDR1 in bronchial epithelial cell culture models are conflicting [1]. Passage number and time in culture have recently been shown to impact on MDR1 expression or activity in ALI bronchial epithelial layers [6,13,14], which may partly explain discrepancies between studies.

Identifying the transporter protein involved in carrier-mediated drug trafficking is highly challenging in biological systems expressing multiple transporters with broad and overlapping substrate specificities. For instance, the cardiac glycoside digoxin has been well characterised as an MDR1 substrate and is largely used for evaluating the risk of drug–drug interactions with new chemical entities consequent to their modulation of MDR1 activity [15,16]. Accordingly, although not an inhaled drug, digoxin has been used for probing MDR1 activity in bronchial cell culture models [13] and in rodent lungs [13,17]. However, digoxin has also been described as a substrate for carriers other than MDR1. These belong to both families of ABC efflux pumps and organic anion transporting polypeptide uptake transporters (OATP; gene symbol: SLCO), namely MDR3 [18]; OATP1B3 [19] and OATP4C1 [20,21]. Conversely, more recent studies have shown OATP1B3, as well as OATP1A2, OATP1B1 and OATP2B1, do not transport digoxin [22,23]. In addition, it is now largely acknowledged that chemical inhibitors commonly used in functional or mechanistic studies, including those originally thought to be specific, actually interact with multiple transporters [24,25].

In this context, our aim was to characterise the bidirectional transport of digoxin in ALI bronchial epithelial cell layers in order to evaluate the contribution of the MDR1 efflux pump and thus the reliability of the drug as a MDR1 probe in such models. To assist in the analysis of *in vitro* permeability data, the expression of a range of transporter genes was initially profiled in the cell culture models. After confirmation of the presence of the MDR1 protein in bronchial epithelial cell layers, the impact of a panel of chemical, immunobiological and metabolic inhibitors on digoxin apparent efflux was investigated in an attempt to identify the transporter involved. Layers of Madin–Darby canine kidney epithelial (MDCKII) cells transfected with the human MDR1 transporter and their wild type counterparts were used for comparison throughout the study.

2. Materials and methods

2.1. Cell culture

Unless otherwise stated, all reagents were purchased from Sigma–Aldrich, UK. The human cancerous bronchial epithelial cell line Calu-3 was obtained from the ATCC (Rockville, MD, USA) and used at a 'low' (25–30) or 'high' (45–50) passage number. Cells were maintained as previously described [13]. For experiments, they were seeded at a density of 1×10^5 cells/cm^2 on 12 well 0.4 μm pore size polyester Transwell® cell culture supports (Corning Costar, High Wycombe, UK). Cells were raised to the air–liquid interface (ALI) after 24 h and maintained on filters for 21 days prior to experimentation.

Normal human bronchial epithelial (NHBE) cells (Lonza, Slough, UK) were cultured using the Lonza proprietary B-ALI® kit according to the manufacturer's instructions. Cells at passage number 2 were seeded at a density of 1.5×10^5 cells/cm^2 onto 0.33 cm^2 polyester Transwell® cell culture supports (Corning Costar) pre-treated with 30 μg/ml rat tail type 1 collagen (Calbiochem, Nottingham, UK). The medium was replaced on the following day, and after 72 h, cells were raised to the ALI. The medium was thereafter changed every 2–3 days, and cell layers were used after 21 days at the ALI.

The human cancerous colonic epithelial cell line Caco-2 and the human embryonic kidney HEK293 cell line were obtained from the ATCC. Wild type and MDR1 transfected Madin–Darby Canine Kidney (MDCKII-WT and MDCKII-MDR1) cells were purchased from the Netherlands Cancer Institute (NKI-AVL, Amsterdam, Netherlands). All cells were cultured in DMEM supplemented with 10% % v/v foetal bovine serum, 100 IU/ml penicillin-100 μg/ml streptomycin solution, 2 mM L-glutamine and 1% v/v non-essential amino acids. Cells were seeded at a density of 2×10^5 cells/cm^2 on 12 well polyester Transwell® cell culture supports and cultured under submerged conditions for 5 (HEK293, MDCKII) or 21 (Caco-2) days.

2.2. Gene expression analysis

Calu-3 and NHBE cell layers were harvested from Transwell® inserts on the same day as ^{3}H-digoxin permeability experiments. mRNA isolation and cDNA synthesis were performed as described previously [26].

Manual TaqMan® analysis of the ABCC7 and ABCC10-12 genes was performed in triplicate in a 25 μl reaction mixture containing 30 ng cDNA, TaqMan® Universal PCR Master Mix (containing AmpliTaq Gold DNA polymerase, dNTPs with dUTP, passive reference and optimised buffer) and Assay-on-demand™ gene expression assay mix (containing 18 μM random hexamer primers). All other genes investigated were analysed via automated Taqman® PCR low density arrays using custom designed 384-well cards as described previously [26]. Amplification curves were analysed using the SDS2.1 software (Applied Biosystems, Foster City, CA) and thresholds for generation of C_T data were calculated automatically by the software. Target genes were compared with the two housekeeping genes RPLP0 (Large Ribosomal Protein) and MVP (Major Vault Protein) ΔC_T and assigned arbitrary categories for relative gene expression levels based on the $2_T^{-\Delta C}$ value, i.e. relative expression levels >0.5 were considered as 'high' (+++), 0.02–0.5 as 'moderate' (++), 0.001–0.02 as 'low' (+) and <0.001 as 'negligible' (−).

2.3. Western blotting

Cells were detached from the surface of the filters/flasks by the addition of 500 μl non-enzymatic cell dissociation buffer prepared in HBSS without calcium and magnesium salts. Cells were counted and resuspended in RIPA cell lysis buffer containing 1 μl of protease inhibitor cocktail set II per 200 μl (ratio of 20 million cells per 1 ml buffer solution) and agitated at 700 rpm at 4 °C for 30 min. Cell debris was pelleted at room temperature by centrifugation at 12,000g for 20 min and the resulting supernatant decanted. Protein concentration was quantified using the RC DC™ protein assay (BioRad, Hemel Hempstead, Hertfordshire).

Protein samples were resolved using 7% Tris–acrylamide gels. Briefly, 10 μl of cell lysate solution containing 20–30 μg of protein was diluted 1:1 with reducing sample buffer. Samples were run under denatured and reduced conditions alongside 5 μl precision plus protein standards (BioRad, Hemel Hempstead, UK) and resolved at 0.04 amps in running buffer.

Transfer to a nitrocellulose membrane was conducted for 60 min at 100 V and at a temperature of 4 °C. Proteins transferred onto Western blots were visualised by staining with copper phthalocyanine 3,4′,4″,4‴-tetrasulphonic acid tetrasodium salt (CPTA). Samples were probed for the presence of MDR1 protein using 5 μg/ml of the mouse anti P-glycoprotein C219 primary antibody (Calbiochem, Nottingham, UK) for 16 h at 4 °C. All steps were performed using a chemiluminescence detection kit according to the manufacturer's instructions (Invitrogen, Paisley, UK).

2.4. Immunohistochemistry

Cell layers were probed for MDR1 protein expression on the same day as functional experiments. Cell layers were rinsed twice

with PBS before being fixed with 3.7% w/v paraformaldehyde for 15 min. Fixed cell layers were permeabilised using 0.1% v/v Triton X-100 in PBS for 5 min and rinsed in PBS. Samples were blocked for 30 min with 1% w/v bovine serum albumin (BSA) in PBS to prevent non-specific binding, followed by incubation with the primary mouse anti-human MDR1 antibodies: 15 µg/ml MRK16 (Abnova, Newmarket, UK) or 20 µg/ml UIC2 (Enzo Life Sciences, Exeter, UK) in blocking solution for 60 min at 37 °C. Cells were washed in 1% w/v BSA in PBS to remove unbound primary antibody before incubation with a solution of the secondary FITC-labelled goat anti-mouse IgG (1:64) in PBS, for a further 30 min. Cell nuclei were counter-stained with propidium iodide (PI) 1 µg/ml in PBS for 30 s. Inserts were washed with PBS before the filter was excised and mounted on a slide using DABCO anti-fade mounting media. Samples were imaged by a Meta 510 confocal microscope (Zeiss, Welwyn Garden City, UK), excited at 485 nm and 543 nm wavelengths and emission observed at 519 nm and 617 nm for FITC and PI, respectively. *Z*-stack reconstructions of samples were the average of four images for every 0.5 µm slice through the sample.

2.5. Flow cytometry

On the day of ^{3}H-digoxin transport studies, cells were detached from Transwell® inserts using trypsin and resuspended in 0.5% v/v FBS in PBS. The cell suspension was adjusted to 1 million cells/ml and 100 µl samples were transferred to clean flow cytometry tubes. Primary anti-MDR1 antibodies (either MRK16 (1 µg) or UIC2 (0.2 µg)) were added and samples incubated at 37 °C for 30 min. Cells were washed and pelleted in cold 'stop solution' (0.5% v/v FBS and 0.1% w/v sodium azide in PBS). The supernatant was decanted, and cells were resuspended in 100 µl 'stop solution' containing FITC-labelled goat anti-mouse IgG (1:1000) and incubated at 4 °C for 30 min. After two PBS wash steps to remove any unbound secondary antibody, samples were fixed by the addition of 500 µl fixing solution (0.5% v/v formaldehyde in PBS) and stored at 4 °C in the dark for up to 1 week before analysis. An unstained sample and the appropriate isotype controls were included in each analysis to address autofluorescence and non-specific binding, respectively.

For data analysis, each sample population was gated to only include cells of interest based on either their forward scatter (cell size) and/or side scatter (cell granularity) profiles. Dead cells were identified from optimisation experiments with PI and excluded from the analysis. A total of 30,000 events were collected for each sample. Raw data were analysed using WinMDI 2.9 software (build #2, 6-19-2000; Scripps Research Institute: http://facs.scripps.edu/software.html) and the mean fluorescence intensity (MFI) value was determined as MFI = [MFI value for sample] − [MFI value for isotype/unstained sample] for each marker.

The UIC2 shift assay was performed as described previously [27]. Samples were treated as outlined above, but first incubated at room temperature for 10 min either alone in 0.5% v/v FBS in PBS or in presence of the chemical inhibitors PSC833 (1 µM) or MK571 (30 µM), before the addition of the UIC2 primary antibody (2 µg/ml). The relative MFI was calculated as the ratio between the MFI of the sample (treated with inhibitor) against the MFI of the cells alone.

2.6. Transport studies

Permeability experiments were conducted using 25 nM ^{3}H-digoxin (Perkin Elmer, Cambridge, UK) in 5 day (MDCKII cells) or 21 day (Calu-3 and NHBE cells) old cell layers in the apical to basolateral (AB) and basolateral to apical (BA) directions in quadruplicate. ^{14}C-mannitol (6.55 µM, Perkin Elmer) was used in all experiments as a marker of epithelial barrier integrity. Cell layers

were allowed to equilibrate at 37 °C for 60 min in standard buffer solution (SBS) comprising HBSS supplemented with 20 mM 4-(2-hydroxyethyl)-1-piperazineethanesulfonic acid (HEPES) and 1% v/v dimethyl sulfoxide (DMSO) in presence or absence of the inhibitors PSC833 (1 µM), MK571 (30 µM) or sodium azide (15 mM). Trans-epithelial electrical resistance (TEER) measurements were taken using an EVOMmeter with chopstick electrodes (World Precision Instruments, Stevenage, UK) and only bronchial epithelial cell layers with a TEER > 300 Ω cm^2 were accepted for experiments. Permeability studies were then carried out as previously detailed [13] maintaining the concentration of substrate, paracellular marker and inhibitors constant throughout the experiments. Cells were maintained at 37 °C and rotated at 60 rpm on an orbital shaker with the exception of temperature dependent studies where the samples were maintained at 4 °C. For biochemical inhibition assays, cell layers were first incubated in SBS containing the mouse anti-human MDR1 antibodies (20 µg/ml UIC2 or 15 µg/ml MRK16) for 60 min at 37°. This was then removed prior to conducting the transport experiments as outlined above. The TEER was measured again at the end of the transport studies to verify the integrity of the cell layers. All samples were mixed with 2 ml Opti-Phase HiSafe 2 scintillation cocktail (Perkin Elmer, Cambridge, UK) and counted using a Wallac 1490 liquid scintillation counter (Wallac, Turku, Finland).

Apparent permeability coefficients (P_{app}) were calculated using the following equation: $P_{app} = \frac{dQ/dt}{AC_0}$ where dQ/dt is the flux of the substrate across the cell layer, A is the surface area of the filter and C_0 is the initial concentration of the substrate in the donor solution.

Cell layers with ^{14}C-mannitol P_{app} values >1.5×10^{-6} cm/s were excluded from the analysis. Efflux ratios were calculated as the ratio of the secretory (BA)/absorptive (AB) apparent permeability (P_{app}) values.

2.7. ATP depletion assay

Calu-3 and MDCKII cell layers were incubated for 3 h in either SBS alone or in SBS containing 15 mM sodium azide. No significant reduction in TEER values was observed at the end of the exposure time. Cells were then assayed for ATP content using the ATP-lite® kit (Perkin Elmer) according to the manufacturer's instructions with minor amendments. In brief, cells were lysed using 50 µl cell lysis buffer at room temperature on an orbital shaker set at 700 rpm. After 5 min, 100 µl luminescent substrate buffer was added and samples were incubated for a further 5 min at 700 rpm. Samples were then transferred to a black 96 well plate, dark adapted for 10 min and analysed for luminescence. ATP content was expressed as the average % relative to the control (SBS alone; *n* = 3 layers).

2.8. Statistics

Results for permeability data were expressed as mean ± standard deviation. Initial data sets with $n \geqslant 5$ were assessed for normality and the data were shown to fit a normal (Gaussian) distribution. Therefore, normality was assumed for all data sets presented in this study. These were compared using a two-tailed, unpaired Student's *t*-test with Welch correction applied (to allow for unequal variance between data sets). Statistical significance was evaluated at 99% ($p < 0.01$) and 95% ($p < 0.05$) confidence intervals. Data considered to be statistically significantly different from control conditions are represented with ** or *, respectively. All statistical tests were performed using GraphPad InStat® version 3.06.

3. Results

3.1. Transporter gene expression

Recently, the expression of a panel of drug transporters has been mapped by semi-quantitative reverse transcriptase polymerase chain reaction in human airway epithelial cells grown under submerged conditions on tissue culture plates [28]. Comparatively, a quantitative analysis of transporter expression in respiratory cell culture absorption models is currently lacking, whereas this would aid the interpretation of in vitro pulmonary permeability data. Hence, we evaluated the expression of selected drug transporter genes in 21 day old ALI Calu-3 layers at a low (25–30) or high (45–50) passage number as well as in NHBE layers grown in similar conditions for comparison. For the majority of transporters investigated, transcript levels were similar between NHBE and Calu-3 layers with no impact of the cell line passage number (Table 1). When differences in transporter expression were obtained between the in vitro models investigated, these were restricted to one arbitrary category (as defined in the method section). This reveals that, despite being of cancerous origin, Calu-3 layers appear to be a suitable in vitro model in which to investigate broncho-epithelial drug transporters. However, it is noteworthy that ABCB1 (MDR1) expression levels were inconsistent between the three cell culture systems studied. Indeed, they were determined as negligible in NHBE cells, low in Calu-3 cells at a high passage and moderate in low passage Calu-3 layers (Table 1).

3.2. MDR1 protein expression

Three different protein detection techniques and a panel of MDR1 antibodies were employed to confirm the presence of MDR1 in bronchial in vitro permeability models.

Western blotting with the C219 antibody detected a protein band at ~170 kDa for the two positive controls Caco-2 and MDCKII-MDR1 cells which was absent for the negative control cell lines HEK293 and MDCKII-WT (Fig. 1). In comparison, protein bands were observed at ~150 kDa for all Calu-3 cell lysates and were the strongest for cells at a high passage number cultured at the ALI (Fig. 1).

The mouse anti-human MDR1 antibodies UIC2 and MRK16 were subsequently used for immunohistochemistry and flow cytometry. A positive immunohistochemical signal was obtained with both antibodies on the apical membranes of all but HEK293 cell layers investigated (Fig. 2). This was however discontinuous on NHBE and low passage Calu-3 layers (Fig. 2). Both MDCKII-WT and MDCKII-MDR1 cell layers stained positively, possibly due to the cross-reactivity of the antibodies with the canine mdr1 expressed in the cells [29]. Staining appeared nevertheless more intense for the transfected cells.

Flow cytometry using the UIC2 antibody produced a low MFI value of 1.3 with the negative control MDCKII-WT cells, whereas the MDCKII-MDR1 positive cell control generated a MFI value of 7.5, demonstrating the UIC2 antibody reacts specifically with MDR1. At low passage, 36% of Calu-3 cells were shown to express the MDR1 transporter in comparison with 70% at a high passage,

Table 1
Gene expression of selected ABC and SLC transporters in human bronchial epithelial cell layers.

Gene	Protein	Calu-3 low passage	Calu-3 high passage	NHBE	Assay ID	Sequence accession ID
MVP	LRP	++	++	++	Hs00245438_m1	NM_017458
RPLP0	RPLP0	+++	+++	+++	Hs99999902_m1	NM_001002
ABCB1	MDR1	++	+	–	Hs00184500_m1	NM_000927
ABCB4	MDR3	–	–	–	Hs00240956_m1	NM_000443
ABCB11	BSEP	+	–	+	Hs00184824_m1	NM_003742
ABCC1	MRP1	++	++	++	Hs00219905_m1	NM_004996
ABCC2	MRP2	+	+	+	Hs00166123_m1	NM_000392
ABCC3	MRP3	++	++	++	Hs00358656_m1	NM_003786
ABCC4	MRP4	+	+	+	Hs00195260_m1	NM_005845
ABCC5	MRP5	++	++	++	Hs00194701_m1	NM_005688
ABCC6	MRP6	+	+	–	Hs00184566_m1	NM_001171
ABCC10	MRP7	++	++	++	Hs00375701_m1	NM_033450
ABCC11	MRP8	–	–	–	Hs00261567_m1	NM_032583
ABCC12	MRP9	–	–	–	Hs00264354_m1	NM_033226
ABCC7	CFTR	++	++	+	Hs00357011_m1	NM_000492
ABCG2	BCRP	–	–	+	Hs00184979_m1	NM_004827
SLC15A1	PEPT1	+	–	++	Hs00192639_m1	NM_005073
SLC15A2	PEPT2	+	–	++	Hs00221539_m1	NM_021082
SLC22A1	OCT1	++	+	+	Hs00427550_m1	NM_153187
SLC22A2	OCT2	–	–	–	Hs00533907_m1	NM_153191
SLC22A3	OCT3	+	+	++	Hs00222691_m1	NM_021977
SLC22A4	OCTN1	–	–	–	Hs00268200_m1	NM_003059
SLC22A5	OCTN2	++	+	++	Hs00161895_m1	NM_003060
SLC22A6	OAT1	–	–	–	Hs00537914_m1	NM_153276
SLC22A7	OAT2	–	–	–	Hs00198527_m1	NM_153320
SLC22A8	OAT3	–	–	–	Hs00188599_m1	NM_004254
SLC22A9	OAT4	–	–	–	Hs00218486_m1	NM_018484
SLCO1A2	OATP1A2	–	–	–	Hs00366488_m1	NM_134431
SLCO1B1	OATP1B1	–	–	–	Hs00272374_m1	NM_006446
SLCO1B3	OATP1B3	++	++	+	Hs00251986_m1	NM_019844
SLCO1C1	OATP1C1	–	–	–	Hs00213714_m1	NM_017435
SLCO2B1	OATP2B1	–	–	–	Hs00200670_m1	NM_007256
SLCO3A1	OATP3A1	++	++	++	Hs00203184_m1	NM_013272
SLCO4A1	OATP4A1	++	++	++	Hs00249583_m1	NM_016354
SLCO4C1	OATP4C1	++	+	++	Hs00698884_m1	NM_180991

Signal intensity represented as: – (<0.001) 'negligible expression'; + (0.001–0.02) 'low expression', ++ (0.02–0.5) 'moderate expression, +++ (>0.5) 'high expression as compared to the two house-keeping genes RPLP0 and MVP.
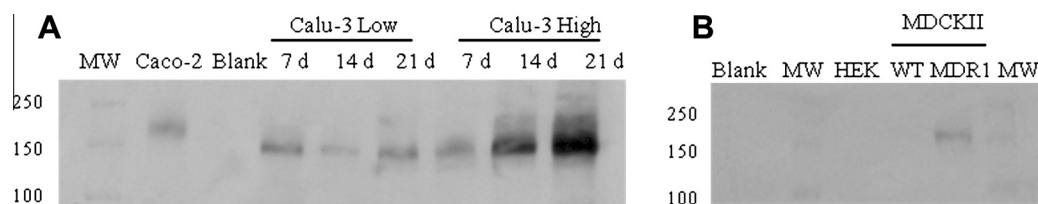
Fig. 1. Detection of MDR1 protein by Western blotting. (A) Calu-3 cell lysates at low and high passage cultured in flasks for 7 days or on Transwell® at the ALI for 14 or 21 days. Caco-2 cell lysate was used as a positive control. (B) MDCKII-MDR1, MDCKII-WT and HEK293 lysates from cells cultured in flasks for 5 days. Samples were run alongside molecular weight markers (MW) and a blank control (lysis and loading buffer solutions only).
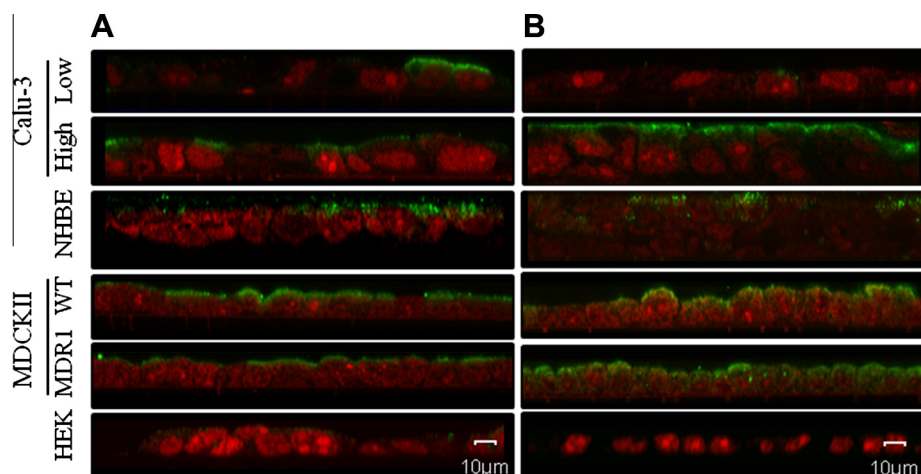

Fig. 2. Confocal laser scanning micrographs of indirect immunofluorescent staining for MDR1 in NHBE cell layers and Calu-3 cells at both low and high passage. All cells were cultured on Transwell® at an ALI for 21 days. MDCKII-MDR1 and HEK293 cells were used as MDR1 positive and negative controls respectively. Cells were treated with primary antibody (A) UIC2 and (B) MRK16. Images are a z-stack of assembled 0.5 μm perpendicular sections of cell layer(s) taken with 63× oil objective and 1× optical zoom with an average of 4 frames per image. Primary antibodies were labelled with a goat anti-mouse IgG FITC-secondary antibody (green). Nuclear components were counter-stained with propidium iodide (red). Images are displayed with the apical surface of the cell layers uppermost. (For interpretation of the references to colour in this figure legend, the reader is referred to the web version of this article.)

resulting in a MFI of 5.2 and 15.0, respectively (Fig. 3). In contrast, only 6% of NHBE cells expressed MDR1 (MFI = 1.3). Similar trends in MDR1 expression levels were obtained with the MRK16 antibody with, however, lower fluorescence values recorded, likely due to a weaker affinity of this antibody for MDR1 (Fig. S1; Supplementary information).

3.3. MDR1 functionality

The well-established MDR1 substrate digoxin is often used to probe MDR1 in biological systems, both *in vitro* and *in vivo* [13,17]. However, the drug has also been reported to be a substrate for other transporters detected at the gene level in our broncho-epithelial cell layers (e.g. some of the OATP) [20,21]. Hence, in order to verify the functionality of MDR1 in bronchial epithelial cells, we performed an UIC2 antibody shift assay in presence of the potent MDR1 inhibitor PSC833 as an alternative to measuring digoxin efflux ratios. This assay is based on the observation that binding of MDR1 ligands alters the conformation of the transporter, which increases the affinity of the UIC2 antibody for the MDR1 protein and causes a shift in fluorescence intensity [30,31]. Relative MFI values of 1.8 and 1.06 were obtained when MDCKII-MDR1 or MDCKII-WT cells, respectively, were pre-incubated with PSC833, in line with their role as positive and negative controls (Fig. S2; Supplementary information). Values of 1.27 and 1.26 were calculated for Calu-3 cells at a low or high passage, respectively, while NHBE cells produced a relative MFI of 1.16 (Fig. S2; Supplementary information),

indicating the presence of a MDR1 activity in bronchial epithelial cells.

3.4. ^{3}H-digoxin bidirectional transport

^{3}H-digoxin permeability measurements were performed in both absorptive (AB) and secretory (BA) directions in MDCKII, Calu-3 and NHBE cell layers.

Both MDCKII-WT and MDCKII-MDR1 cell layers displayed a net secretory transport of ^{3}H-digoxin (Fig. 4) which was significantly reduced ($p < 0.01$) at 4 °C (Fig. S3; Supplementary information). The presence of an apparent efflux mechanism in the two cell types was allegedly ascribed to the activity of the canine mdr1 transporter in MDCKII cells [29]. As predicted, ^{3}H-digoxin efflux ratio was significantly higher ($p < 0.01$) in transfected cells (Fig. 4), reflecting the involvement of the human MDR1 transporter in ^{3}H-digoxin asymmetric transport in the cell line.

A large degree of variability in ^{3}H-digoxin permeability values was observed between the two batches of NHBE cells employed, despite originating from the same donor (Fig. 4). Accordingly, a range of efflux ratios between 1.0 and 2.3 were calculated for the two batches tested under identical culture conditions, questioning the presence of an efflux mechanism for digoxin in NHBE layers. Although within the acceptable range, ^{14}C-mannitol BA permeability values were significantly different ($p < 0.05$) between the two batches, which might have contributed to the variations in ^{3}H-digoxin secretory transport obtained.
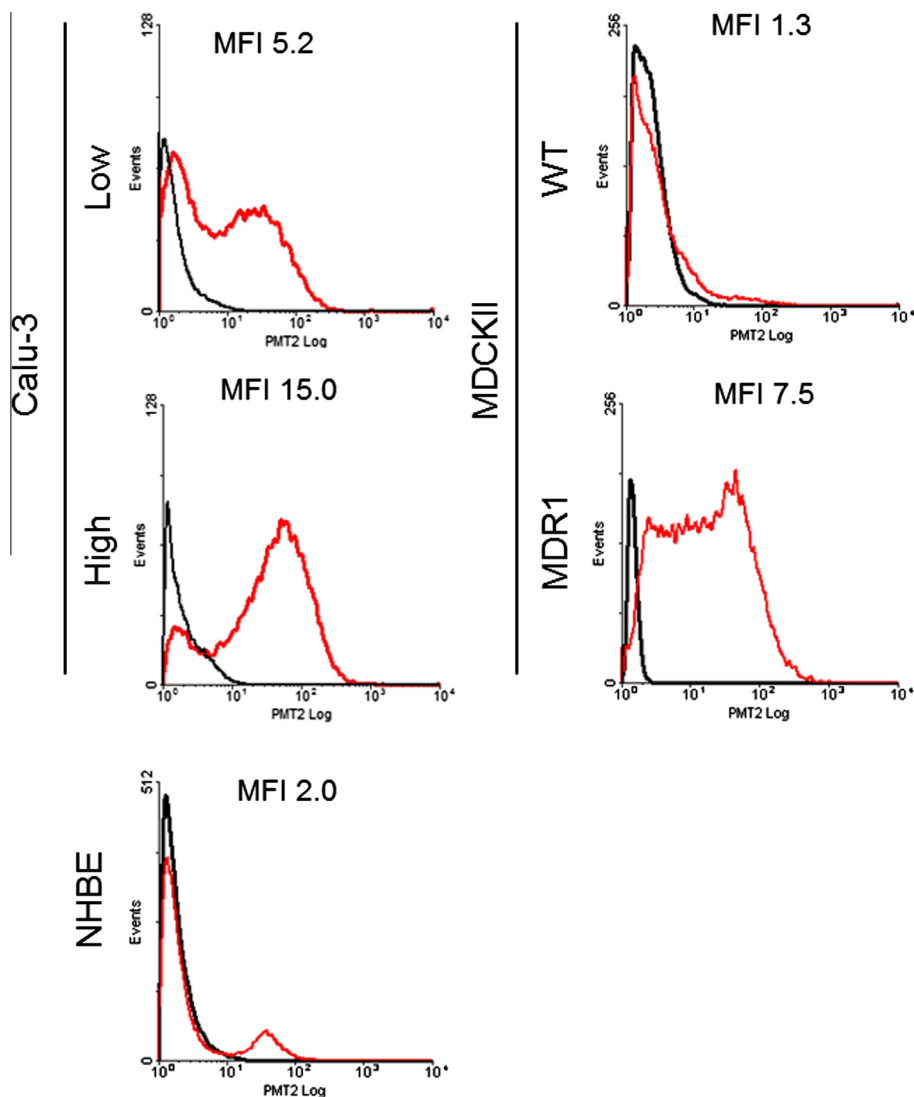
Fig. 3. Detection of MDR1 protein expression by flow cytometry in NHBE cell layers and Calu-3 cell layers at high and low passage. All cells were cultured on filters at an ALI for 21 days. MDCKII-WT and MDCKII-MDR1 cells were included as negative and positive MDR1 controls, respectively. Data are displayed for 3×10^5 events showing the secondary control (black) and sample incubated with 0.2 µg/100 µl UIC2 mouse anti-human MDR1 antibody and labelled with 1:1000 goat anti-mouse IgG FITC-tagged secondary antibody (red). Relative MFI (sample MFI/control MFI) are stated for each cell type. (For interpretation of the references to colour in this figure legend, the reader is referred to the web version of this article.)
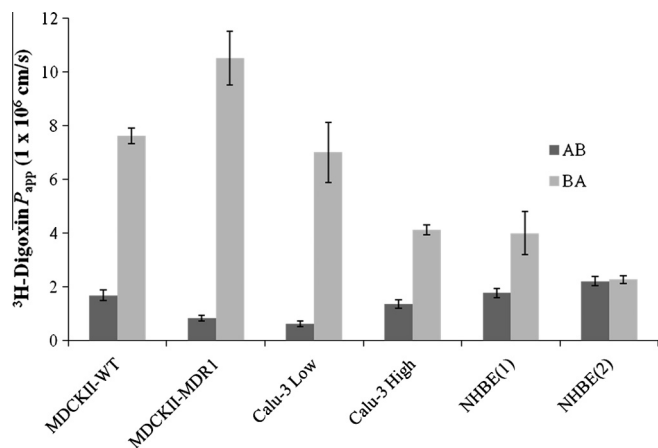

Fig. 4. Transport of 25 nM ^{3}H-digoxin across epithelial cell layers in both absorptive (AB) and secretory (BA) directions. Calu-3 cells and NHBE cell layers were cultured at an ALI for 21 days and MDCKII cells were cultured for 5 days under submerged conditions. Data are represented as the mean ± SD of 4 layers.

Net secretory transport of ^{3}H-digoxin was observed in both low and high passage Calu-3 layers, but with a higher efflux ratio measured at a low passage number (Fig. 4). ^{3}H-digoxin asymmetric transport was abolished at 4 °C (Fig. S3; Supplementary information), confirming the involvement of a transporter-mediated mechanism.

3.5. Impact of inhibitors on ^{3}H-digoxin bidirectional transport

In order to evaluate the contribution of MDR1 to digoxin trafficking in MDCKII and Calu-3 layers, inhibition studies were performed with PSC833 (1 µM), the two specific MDR1 inhibitory antibodies UIC2 (20 µg/ml) and MRK16 (15 µg/ml) as well as MK571 (30 µM), an inhibitor of the multidrug resistance proteins (MRP) [32] which had previously been reported not to inhibit MDR1 even at a higher concentration of 50 µM [33]. Considering the poor reproducibility of transport data in NHBE layers, inhibition studies were not performed in this model.

Table 2
Impact of inhibitors on ^{3}H-digoxin bidirectional transport.

^{3}H-digoxin P_{app} (1×10^{-6} cm/s)				
	AB	Significance	BA	Significance
PSC833 1 µM				
MDCKII-WT	1.31 ± 0.18	↔	1.25 ± 0.10	↓ **
MDCKII-MDR1	0.78 ± 0.03	↑ **	3.51 ± 0.21	↓ **
Calu-3 Low	2.02 ± 0.22	↑ **	2.44 ± 0.10	↓ **
Calu-3 High	1.10 ± 0.08	↑ **	1.50 ± 0.32	↓ **
UIC2 20 µg/ml				
MDCKII-WT	0.97 ± 0.16	↔	5.56 ± 0.33	↔
MDCKII-MDR1	0.52 ± 0.05	↑ **	7.43 ± 0.28	↓ *
Calu-3 Low	0.20 ± 0.03	↓ **	7.97 ± 1.08	↔
Calu-3 High	1.49 ± 0.13	↔	4.24 ± 0.32	↔
MRK16 15 µg/ml				
MDCKII-WT	0.90 ± 0.06	↔	5.54 ± 0.05	↔
MDCKII-MDR1	0.45 ± 0.03	↔	6.88 ± 0.40	↓ **
Calu-3 Low	0.63 ± 0.04	↔	4.43 ± 0.20	↓ *
Calu-3 High	1.58 ± 0.03	↔	4.21 ± 0.15	↔
MK571 30 µM				
MDCKII-WT	2.09 ± 0.12	↑ **	7.25 ± 0.65	↔
MDCKII-MDR1	1.35 ± 0.02	↑ **	7.39 ± 0.53	↔
Calu-3 Low	1.61 ± 0.05	↑ **	3.70 ± 0.31	↓ **
Calu-3 High	1.77 ± 0.14	↑ **	2.31 ± 0.07	↓ **

Data are presented as mean ± SD (n = 4 layers). ↔ indicate no statistical difference ($p > 0.05$) and ↑↓ a statistically significant increase or decrease compared to permeability values obtained in the same experimental conditions in absence of inhibitors. AB: apical to basolateral; BA: basolateral to apical.
* $p < 0.05$.
** $p < 0.01$.

PSC833 significantly decreased ^{3}H-digoxin secretory transport in all cell layers under investigation, reducing or abolishing its apparent efflux (Table 2). This suggested an involvement of MDR1/mdr1 in the drug transport in both cell lines. Nevertheless, this was not confirmed by functional inhibitory studies with the UIC2 and MRK16 antibodies.

Both antibodies are MDR1 specific probes that react with extracellular loops of the transporter, fixing it in a conformational state and thus altering the binding of its substrates [30,31]. As anticipated, the antibodies had no significant impact on ^{3}H-digoxin trafficking in MDCKII-WT cells, but significantly decreased ^{3}H-digoxin BA P_{app} in MDCKII-MDR1 layers (Table 2). None of the antibodies affected ^{3}H-digoxin permeability in Calu-3 cells at a high passage number (Table 2). A small but statistically significant decrease in BA ^{3}H-digoxin transport was observed in Calu-3 layers at a low passage number with the MRK16 antibody, whereas the UIC2 clone had no impact on the drug secretory transport in these layers (Table 2).

MK571 enhanced ^{3}H-digoxin absorptive transport in all cell types but only reduced the drug secretory permeability in Calu-3 cell layers (Table 2). A relative MFI of 1.05 was obtained in an UIC2 antibody shift assay performed in MDCKII-MDR1 cells incubated with MK571, confirming the compound does not bind to MDR1.

Table 3
Impact of 3 h incubation in presence of sodium azide (15 mM) on ATP cellular levels.

	% ATP relative to control
MDCKII-WT	17.6 ± 4.0
MDCKII-MDR1	28.8 ± 6.8
calu-3 low	48.6 ± 7.0
Calu-3 high	53.7 ± 5.3

Data are presented as mean ± SD (n = 3 layers).

Table 4
Impact of sodium azide (15 mM) on ^{3}H-digoxin bidirectional transport.

^{3}H-digoxin P_{app} (1×10^{-6} cm/s)				
	AB	Significance	BA	Significance
MDCKII-WT	1.03 ± 0.09	↔	4.92 ± 0.40	↔
MDCKII-MDR1	0.52 ± 0.07	↑ *	5.12 ± 0.20	↓ **
Calu-3 Low	0.28 ± 0.02	↔	8.03 ± 0.12	↔
Calu-3 High	0.86 ± 0.03	↔	3.64 ± 0.14	↓ *

Data are presented as mean ± SD (n = 4 layers). ↔ indicate no statistical difference and ↑↓ a statistically significant increase or decrease compared to permeability values obtained in the same experimental conditions in absence of sodium azide. AB: apical to basolateral; BA: basolateral to apical.
* $p < 0.05$.
** $p < 0.01$.

3.6. Impact of ATP depletion on ^{3}H-digoxin bidirectional transport

Since ABC transporters are ATP-dependent, the effect of a reduction of ATP cellular levels on ^{3}H-digoxin P_{app} in MDCKII and Calu-3 layers was finally assessed.

Incubation with 15 mM sodium azide for 3 h induced a ~70–80% and ~50% ATP depletion in MDCKII or Calu-3 layers, respectively (Table 3). Interestingly, no significant effect of the metabolic inhibitor on digoxin permeability was observed in MDCKII-WT (Table 4), which is in contradiction with a presumed role of the canine mdr1 in the drug apparent efflux in the cell culture model. In contrast, decreased ATP production in MDCKII-MDR1 resulted in an enhanced or reduced digoxin transport in the absorptive or secretory directions, respectively (Table 4). Moreover, in these conditions, BA transport was not significantly different ($p > 0.05$) from that in the wild type cell layers, suggesting complete inhibition of the MDR1 transporter. Reduction in ATP levels in Calu-3 layers did not affect ^{3}H-digoxin apparent efflux at a low passage number but decreased the BA transport by ~10% at a higher passage number (Table 4).

4. Discussion

Due to the complexity of the lungs, ALI human bronchial epithelial cell layers are becoming popular systems for investigating drug-transporter interactions in the airway epithelium [1,7]. However, the expression and functionality of most transporters have yet to be meticulously characterised in these models. In particular, the presence and activity of the MDR1 efflux pump in NHBE and Calu-3 layers remain controversial to date [1]. This may be explained by inter-laboratory variations in culture conditions but equally attributed to the use of non-specific substrates and inhibitors in functional studies.

This study characterised MDR1 expression and the bidirectional transport of the MDR1 probe digoxin in layers of NHBE and the Calu-3 cell line at low (25–30) or high (45–50) passage numbers using MDCKII-MDR1 and wild type equivalents for comparison.

MDR1 expression data obtained by three independent protein detection techniques using three different MDR1 antibodies were in agreement and indicated a weak presence of the transporter in NHBE cells as well as an increased expression at a high passage number in Calu-3 cells (Figs. 1–3). Surprisingly, protein expression levels in the cell line were in contradiction with the higher ABCB1 transcript levels measured at an early passage number (Table 1). This highlights the importance of investigating transporter expression at the protein level in complement to gene profiling for a reliable appraisal of their presence in the cell culture system under investigation as well as unbiased interpretation of functional data. Western blotting revealed a protein band for Calu-3 samples at a molecular weight ~20 kDa lower than for Caco-2 and

MDCKII-MDR1 cells (Fig. 1). Hamilton and colleagues [34] also obtained a band ~150 kDa in Calu-3 cells using the same C219 antibody. This clone is known to react with MDR3 (~150 kDa) as well as with MDR1. However, no ABCB4 (MDR3) transcripts were detected in the cell line (Table 1), in agreement with the absence of this transporter in human airway epithelium samples [35]. More plausible causes for the presence of a band at a molecular weight lower than expected could include impaired post-translational modifications such as a different degree of glycosylation in Calu-3 cells. The impact of glycosylation on MDR1functionality is not completely understood to date with studies having reported either an uncompromised efflux activity [36,37] or conversely, a diminished function [38,39] of the non-glycosylated transporter. It had also been postulated that glycosylation was crucial for correct folding of the MDR1 protein into the cell membrane [40]. However, a shift assay performed with the conformation sensitive IUC2 antibody on Calu-3 cells demonstrated that the efflux pump expressed in the cell line was capable of binding the PSC833 inhibitor and modifying its conformation following ligand recognition (Fig. S2, Supplementary info) similarly to a non-glycosylated MDR1 mutant in presence of the inhibitor cyclosporin A [36]. This indicated that, despite a possible altered structure, MDR1 was functional in the Calu-3 cell line.

The ^{3}H-digoxin apparent efflux ratio measured in NHBE layers was poorly reproducible and was therefore not investigated further (Fig. 4). In Calu-3 layers, this was higher at a low passage (Fig. 4) whereas MDR1 protein expression levels were greater in cells at a high passage number (Figs. 1–3). ^{3}H-digoxin transport was not affected by ATP depletion at low passage and only marginally at a high passage number (Table 4). Furthermore, the two MDR1 specific inhibitory antibodies MRK16 and IUC2 had no impact on the drug trafficking in high passage Calu-3 layers while the MRK16 clone alone decreased BA transport at a low passage number (Table 2). The extent of MDR1 inhibition by MRK16 and UIC2, although specific, has been described as partial (10–40%) and largely dependent on the substrate under investigation [41]. Assuming that the ^{3}H-digoxin permeability in the secretory direction in MDCKII-MDR1 cells above that in their wild type counterparts is the component mediated by the transfected human efflux pump, a ~20% and ~30% reduction in MDR1 mediated digoxin transport was obtained with the UIC2 and MRK16 antibodies, respectively, which validated the experimental protocol followed. Finally, MK571 increased ^{3}H-digoxin absorptive transport in both MDCKII and Calu-3 layers but only reduced its secretory transport in the bronchial cell line (Table 2). In contrast, the drug permeability in the BA direction was decreased in presence of PSC833 in all cell layers (Table 2). In addition to its inhibitory properties on various MRP carriers [32], MK571 has been recently reported to interfere with the activity of OATP1B3 and OATP2B1 at a concentration as low as 1 μM [42,43]. Its modulatory effects on other OATP transporters present in Calu-3 layers (Table 1) are currently unknown. Nevertheless, the compound has been shown not to interact with MDR1 [33], which we confirmed in an IUC2 shift assay. Although PSC833 was originally developed as a specific MDR1 inhibitor, it has since been reported to inhibit other ABC transporters, such as the bile salt extrusion pump (BSEP) [44], MRP2 [45] or the breast cancer resistance protein (BCRP, Solvo Biotech website) and its ability to inhibit OATP transporters has been suggested [46].

Taken together, ^{3}H-digoxin permeability data in Calu-3 layers do not support an exclusive participation of the MDR1 transporter in its apparent efflux and suggest the involvement of one or several ATP-independent transport system(s). Similarly, it has previously been demonstrated that MDR1 was not the sole transporter responsible for digoxin asymmetric transport in the Caco-2 intestinal absorption model [33] and in MDR1 transfected MDCK cell layers [47].

Although this/these transporter(s) remain(s) to be identified, OATP4C1 might be a possible candidate since digoxin is a known substrate [20,21], the transporter is present in Calu-3 layers and a lower gene expression was observed at a high passage number (Table 1). Assuming protein levels are in agreement with those of mRNA transcripts, this could explain the reduced digoxin apparent efflux in high passage cell layers. This assumption implies a basolateral location of OATP4C1 in Calu-3 layers in line with the basolateral presence of OATP transporters that has been recently postulated in the airway epithelium of foals [48]. However, there remains a possibility that digoxin is transported across bronchial epithelial cell layers by a transporter yet to be characterised, as suggested in other cell culture models [22,23,47]. For instance, in addition to the apical MDR1 efflux pump, a basolaterally located uptake transporter was required to account for digoxin net secretory transport in MDCKII-MDR1 cell layers but this transporter could not be identified using a panel of inhibitors [47]. As previously debated for the MDCKII-MDR1 absorption model [47], the likely involvement of multiple transporters in digoxin bidirectional transport in Calu-3 layers questions its suitability for probing MDR1 activity in the bronchial epithelium.

5. Conclusions

This study exemplifies the complexity of analysing in vitro permeability data obtained with substrates of multiple transporters and highlights the need for thorough characterisation of transporter expression in cell based drug absorption models. The sole participation of MDR1 in digoxin net secretory transport in Calu-3 layers could not be demonstrated and the contribution of an ATP-independent transporter such as a basolaterally located member of the OATP family was therefore hypothesised. Identification of this unknown transporter might provide a better understanding of the distribution of drugs in the pulmonary tissue.

Appendix A. Supplementary material

Supplementary data associated with this article can be found, in the online version, at http://dx.doi.org/10.1016/j.ejpb.2013.06.010.

References

[1] C. Bosquillon, Drug transporters in the lung – do they play a role in the biopharmaceutics of inhaled drugs?, J Pharm. Sci. 99 (2010) 2240–2255.
[2] B. Forbes, B. Asgharian, L. Dailey, D. Fergurson, P. Gerde, M. Gumbleton, L. Gustavsson, C. Hardy, D. Hassall, R. Jones, Challenges in inhaled product development and opportunities for open innovation, Adv. Drug. Deliv. Rev. 63 (2011) 69–87.
[3] J.L. Sporty, L. Horálková, C. Ehrhardt, In vitro cell culture models for the assessment of pulmonary drug disposition, Expert. Opin. Drug. Metab. Toxicol. 4 (2008) 333–345.
[4] B. Forbes, C. Ehrhardt, Human respiratory epithelial cell culture for drug delivery applications, Eur. J. Pharm. Biopharm. 60 (2005) 193–205.
[5] C.I. Grainger, L.L. Greenwell, D.J. Lockley, G.P. Martin, B. Forbes, Culture of Calu-3 cells at the air interface provides a representative model of the airway epithelial barrier, Pharm. Res. 23 (2006) 1482–1490.
[6] H. Lin, H. Li, H.J. Cho, S. Bian, H.J. Roh, M.K. Lee, J.S. Kim, S.J. Chung, C.K. Shim, D.D. Kim, Air–liquid interface (ALI) culture of human bronchial epithelial cell monolayers as an in vitro model for airway drug transport studies, J. Pharm. Sci. 96 (2007) 341–350.

[7] M. Mukherjee, D.I. Pritchard, C. Bosquillon, Evaluation of air-interfaced Calu-3 cell layers for investigation of inhaled drug interactions with organic cation transporters in vitro, Int. J. Pharm. 426 (2012) 7–14.

[8] M. Mamlouk, P.M. Young, M. Bebawy, M. Haghi, S. Mamlouk, V. Mulay, D. Traini, Salbutamol sulfate absorption across Calu-3 bronchial epithelia cell monolayer is inhibited in the presence of common anionic NSAIDs, J. Asthma 50 (2013) 334–341.

[9] H.X. Ong, D. Traini, M. Bebawy, P.M. Young, Ciprofloxacin is actively transported across bronchial lung epithelial using a Calu-3 air-interface cell model, Antimicrob. Agents Chemother. (2013) (March 18) (Epub ahead of print).

[10] H. Glaeser, Importance of P-glycoprotein for drug–drug interactions, Handb. Exp. Pharmacol. 201 (2011) 285–297.

[11] B.L. Urquhart, R.B. Kim, Blood–brain barrier transporters and response to CNS-active drugs, Eur. J. Clin. Pharmacol. 65 (2009) 1063–1070.

[12] K. Bleasby, J.C. Castle, C.J. Roberts, C. Cheng, W.J. Bailey, J.F. Sina, A.V. Kulkarni, M.J. Hafey, R. Evers, J.M. Johnson, R.G. Ulrich, J.G. Slatter, Expression profiles of 50 xenobiotic transporter genes in humans and pre-clinical species: a resource for investigations into drug disposition, Xenobiotica 36 (2006) 963–988.

[13] M. Madlova, C. Bosquillon, D. Asker, P. Dolezal, B. Forbes, In-vitro respiratory drug absorption models possess nominal functional P-glycoprotein activity, J. Pharm. Pharmacol. 61 (2009) 293–301.

[14] M. Haghi, P.M. Young, D. Traini, R. Jaiswal, J. Gong, M. Bebawy, Time- and passage-dependent characteristics of a Calu-3 respiratory epithelial cell model, Drug. Dev. Ind. Pharm. 36 (2010) 1207–1214.

[15] J. Rautio, J.E. Humphreys, L.O. Webster, A. Balakrishnan, J.P. Keogh, J.R. Kunta, C.J. Serabjit-Singh, J.W. Polli, In vitro p-glycoprotein inhibition assays for assessment of clinical drug interaction potential of new drug candidates: a recommendation for probe substrates, Drug Metab. Dispos. 34 (2006) 786–792.

[16] S.-M. Huang, R. Temple, D.C. Throckmorton, L.J. Lesko, Drug interaction studies: study design, data analysis, and implications for dosing and labeling, Clin. Pharmacol. Ther. 81 (2007) 298–304.

[17] F. Manford, A. Tronde, A.B. Jeppsson, N. Patel, F. Johansson, B. Forbes, Drug permeability in 16HBE14o-airway cell layers correlates with absorption from the isolated perfused rat lung, Eur. J. Pharm. Sci. 26 (2005) 414–420.

[18] A.J. Smith, A. Van Helvoort, G. Van Meer, K. Szabo, E. Welker, G. Szakacs, A. Varadi, B. Sarkadi, P. Borst, MDR3 P-glycoprotein, a phosphatidylcholine translocase, transports several cytotoxic drugs and directly interacts with drugs as judged by interference with nucleotide trapping, J. Biol. Chem. 275 (2000) 23530–23539.

[19] G.A. Kullak-Ublick, M.G. Ismair, B. Stieger, L. Landmann, R. Huber, F. Pizzagalli, K. Fattinger, P.J. Meier, B. Hagenbuch, Organic anion-transporting polypeptide B (OATP-B) and its functional comparison with three other OATPs of human liver, Gastroenterology 120 (2001) 525–533.

[20] T. Mikkaichi, T. Suzuki, T. Onogawa, M. Tanemoto, H. Mizutamari, M. Okada, T. Chaki, S. Masuda, T. Tokui, N. Eto, M. Abe, F. Satoh, M. Unno, T. Hishinumna, K. Inui, S. Ito, J. Goto, T. Abe, Isolation and characterization of a digoxin and its rat homologue expressed in the kidney, Proc. Natl. Acad. Sci. USA 101 (2004) 3569–3574.

[21] H. Yamaguchi, M. Sugie, M. Okada, T. Mikkaichi, T. Toyohara, T. Abe, J. Goto, T. Hishinuma, M. Shimada, N. Mano, Transport of estrone 3-sulfate mediated by organic anion transporter OATP4C1: estrone 3-sulfate binds to the different recognition site for digoxin in OATP4C1, Drug Metab. Pharmacokinet. 25 (2010) 314–317.

[22] E. Kimoto, J. Chupka, Y. Xiao, Y.A. Bi, D.B. Duignan, Characterization of digoxin uptake in sandwich-cultured human hepatocytes, Drug Metab. Dispos. 39 (2011) 47–53.

[23] M.E. Taub, K.M. Mease, R.S. Sane, C.A. Watson, L. Chen, H. Ellens, B.P. Hirakawa, E.L. Reyner, M. Jani, C.A. Lee, Digoxin is not a substrate for organic anion transporting polypeptide transporters OATP1A2, OATP1B1, OATP1B3, and OATP2B1 but is a substrate for a sodium dependent transporter expressed in HEK293 Cells, Drug Metab. Dispos. 39 (2011) 2093–2102.

[24] Q. Wang, R. Strab, P. Kardos, C. Ferguson, J. Li, A. Owen, I.J. Hidalgo, Application and limitation of inhibitors in drug-transporter interactions studies, Int. J. Pharm. 356 (2008) 12–18.

[25] K. Mease, R. Sane, L. Podila, M.E. Taub, Differential selectivity of efflux transporter inhibitors in Caco-2 and MDCK-MDR1 monolayers: a strategy to assess the interaction of a new chemical entity with P-gp, BCRP, and MRP2, J. Pharm. Sci. 101 (2012) 1888–1897.

[26] C. Hilgendorf, G. Ahlin, A. Seithel, P. Artursson, A. Ungell, J. Karlsson, Expression of thrity-six drug transporter genes in human intestine, liver, kidney and organotypic cell lines, Drug Metab. Dispos. 35 (2007) 1333–1340.

[27] E.B. Mechetner, B. Schott, B.S. Morse, W.D. Stein, T. Druley, K.A. Davis, T. Tsuruo, I.B. Roninson, P-glycoprotein function involves conformational transitions detectable by differential immunoreactivity, Proc. Natl. Acad. Sci. USA 94 (1997) 12908–12913.

[28] S. Endter, D. Francombe, C. Ehrhardt, M. Gumbleton, RT-PCR analysis of ABC, SLC and SLCO drug transporters in human lung epithelial cell models, J. Pharm. Pharmacol. 61 (2009) 583–591.

[29] K. Kuteykin-Teplyakov, C. Luna-Tortós, K. Ambroziak, W. Löscher, Differences in the expression of endogenous efflux transporters in MDR1-transfected versus wildtype cell lines affect P-glycoprotein mediated drug transport, Br. J. Pharmacol. 160 (2010) 1453–1463.

[30] S.W. Park, N. Lomri, L.A. Simeoni, J.P. Fruehauf, E. Mechetner, Analysis of P-glycoprotein-mediated membrane transport in human peripheral blood lymphocytes using the UIC2 shift assay, Cytometry A 53 (2003) 67–78.

[31] E. Mechetner, Detection of the MDR1 P-glycoprotein expression and function, Methods Mol. Biol. 378 (2007) 175–193.

[32] S.F. Zhou, L.L. Wang, Y.M. Di, C.C. Xue, W. Duan, C.G. Li, Y. Li, Substrates and inhibitors of human multidrug resistance associated proteins and the implications in drug development, Curr. Med. Chem. 15 (2008) 1981–2039.

[33] S. Lowes, M.E. Cavet, N.L. Simmons, Evidence for a non-MDR1 component in digoxin secretion by human intestinal Caco-2 epithelial layers, Eur. J. Pharmacol. 458 (2003) 49–56.

[34] K.O. Hamilton, G. Backstrom, M.A. Yazdanian, K.L. Audus, P-glycoprotein efflux pump expression and activity in Calu-3 cells, J. Pharm. Sci. 90 (2001) 647–658.

[35] G.L. Scheffer, A.C.L.M. Pijnenborg, E.F. Smit, M. Müller, D.S. Postma, W. Timens, P. Van Der Valk, E.G.E. De Vries, R.J. Scheper, Multidrug resistance related molecules in human and murine lung, J. Clin. Pathol. 55 (2002) 332–339.

[36] J.J. Gribar, M. Ramachandra, C.A. Hrycyna, S. Dey, S.V. Ambudkar, Functional characterization of glycosylation-deficient human P-glycoprotein using a vaccinia virus expression system, J. Membr. Biol. 173 (2000) 203–214.

[37] M. Sereš, D. Cholujová, T. Bubenčíkova, A. Breier, Z. Sulová, Tunicamycin depresses p-glycoprotein glycosylation without an effect on its membrane localization and drug efflux activity in l1210 cells, Int. J. Mol. Sci. 12 (2011) 7772–7784.

[38] V. Draheim, A. Reichel, W. Weitschies, U. Moenning, N-glycosylation of ABC transporters is associated with functional activity in sandwich-cultured rat hepatocytes, Eur. J. Pharm. Sci. 41 (2010) 201–209.

[39] J. Molnár, M.D. Kars, U. Gündüz, H. Engi, U. Schumacher, E.J. Van Damme, W.J. Peumans, J. Makovitzky, N. Gyémánt, P. Molnár, Interaction of tomato lectin with ABC transporter in cancer cells: glycosylation confers functional conformation of P-gp, Acta Histochem. 111 (2009) 329–333.

[40] R. Kramer, T.K. Weber, R. Arceci, N. Ramchurren, W.V. Kastrinakis, G.Jr. Steele, I.C. Summerhayes, Inhibition of N-linked glycosylation of P-glycoprotein by tunicamycin results in a reduced multidrug resistance phenotype, Br. J. Cancer 71 (1995) 670–675.

[41] K. Goda, F. Fenyvesi, Z. Bacsó, H. Nagy, T. Márián, A. Megyeri, Z. Krasznai, I. Juhász, M. Vecsernyés, G. Szabó, Complete inhibition of P-glycoprotein by simultaneous treatment with a distinct class of modulators and the UIC2 monoclonal antibody, J. Pharmacol. Exp. Ther. 320 (2007) 81–88.

[42] K. Letschert, M. Komatsu, J. Hummel-Eisenbeiss, D. Keppler, Vectorial transport of the peptide CCK-8 by double-transfected MDCKII cells stably expressing the organic anion transporter OATP1B3 (OATP8) and the export pump ABCC2, J. Pharmacol. Exp. Therapy 313 (2005) 356–549.

[43] K. Letschert, H. Faulstich, D. Keller, D. Keppler, Molecular characterization and inhibition of amanitin uptake into human hepatocytes, Toxicol. Sci. 91 (2006) 140–149.

[44] S. Childs, R.L. Yeh, D. Hui, V. Ling, Taxol resistance mediated by transfection of the liver-specific sister gene of P-glycoprotein, Cancer Res. 58 (1998) 4160–4167.

[45] M. Böhme, M. Büchler, M. Müller, D. Keppler, Differential inhibition by cyclosporins of primary-active ATP-dependent transporters in the hepatocyte canalicular membrane, FEBS Lett. 333 (1993) 193–196.

[46] F. Bourasset, S. Cisternino, J. Temsamani, J.M. Scherrmann, Evidence for an active transport of morphine-6-beta-d-glucuronide but not P-glycoprotein-mediated at the blood–brain barrier, J. Neurochem. 86 (2003) 1564–1567.

[47] P. Acharya, M.P. O'Conor, J.W. Polli, A. Ayrton, H. Ellens, J. Bentz, Kinetic identification of membrane transporters that assist P-glycoprotein-mediated transport of digoxin and loperamide through a confluent monolayer of MDCKII-hMDR1 cells, Drug Metab. Dispos. 36 (2008) 452–460.

[48] J. Peters, W. Block, S. Oswald, J. Freyer, M. Grube, H. Kroemer, M. Lämmer, D. Lütjohann, M. Venner, W. Siegmund, Oral absorption of clarithromycin is nearly abolished by chronic comedication of rifampicin in foals, Drug Metab. Dispos. 39 (2011) 1643–1649.